American Mineralogist, Volume 77, pages 1133–1143, 1992

Structural chemistry of Mn, Fe, Co, and Ni in manganese hydrous oxides: Part I. Information from XANES spectroscopy

ALAIN MANCEAU*
Laboratoire de Minéralogie-Cristallographie, Universités Paris 6 et 7, CNRS UA09, Tour 16, 4 place Jussieu, 75252 Paris Cedex 05, France

ANATOLII I. GORSHKOV
Institute of Ore Geology and Mineralogy (IGEM) of the USSR Academy of Science, 35 Staromonetny prospekt, 109017 Moscow, Russia

VICTOR A. DRITS
Geological Institute of the USSR Academy of Science, 7 Pyzhevsky prospekt, 109017 Moscow, Russia

ABSTRACT

The oxidation state and coordination number of Mn, Fe, and Co in hydrous manganese oxides have been investigated by high resolution XANES spectroscopy. At the Mn*K* edge, spectral sensitivity is high enough to differentiate between Mn ions of different oxidation states and site occupations. Application of this technique to various poorly crystallized hydrous oxides, including samples of birnessite, vernadite, asbolane, and manganese goethite, indicates that Mn atoms are generally tetravalent. If low-valence Mn ions are present, they certainly make up less than 20 at%. In natural Fe-containing vernadite, Fe atoms are sixfold coordinated, on the basis of a detection limit for $^{[4]}Fe^{3+}$ ions of about 10 at%. Co has been found to be trivalent in both cobalt and cobalt nickel asbolane. Mn*K* preedge spectra have also been demonstrated to be sensitive to the local structure of tetravalent manganate. Spectral intensity was found to depend on the ratio of edge- to corner-sharing MnO_6 octahedra: the larger the tunnel size of the manganate, the lower the intensity of the preedge. Application of this concept to the structure of δ-MnO_2 suggests that vernadite contains as many corner-sharing octahedra as todorokite. On the basis of XANES data, δ-MnO_2 does not possess a layered structure and should not be considered as long-range disordered birnessite.

INTRODUCTION

In mineral structures, Mn, Fe, and Co atoms can occur in a number of oxidation states and sites. For instance, Mn^{2+}, Mn^{3+}, Fe^{2+}, Fe^{3+}, and Co^{2+} ions can be found in both octahedral and tetrahedral coordinations, whereas Mn^{4+} and low-spin Co^{3+} are restricted to octahedral sites. An understanding of the electronic structure of cations in minerals can be important for constraining structural interpretations from X-ray diffraction (XRD) data. This information is particularly useful for elucidating the structure of poorly crystallized hydrous oxides for which diffraction intensity data fail to provide a unique solution. For example, several models have been proposed for the structure of ferrihydrite. Some researchers have found only sixfold-coordinated Fe atoms (Towe and Bradley, 1967), whereas others have reported significant filling of tetrahedral sites, 33% by Eggleton and Fitzpatrick (1988) to 50% by Harrison et al. (1967). In another instance, Chukhrov et al. (1988) interpreted XRD data from iron vernadite by assuming the presence of about one-third of (Fe,Mn) atoms in fourfold coordination.

The purpose of this work is to more accurately determine the oxidation state and site occupation of Mn, Fe, and Co in various hydrous manganese oxides by using X-ray absorption near-edge structure (XANES) spectroscopy. This crystal chemical information provides constraints for interpreting structural data obtained for the same materials using XRD, selected area electron diffraction (SAED), energy dispersive spectrometry (EDS), and extended X-ray absorption fine structure (EXAFS) spectroscopy. These results are presented and discussed in the second part of this paper (Manceau et al., 1992).

XANES spectra are usually separated into two parts: the preedge and the main-edge regions (Brown et al., 1988). The former is located to the lower energy side of the steeply rising absorption edge and corresponds to 1s → 3d type electronic transitions. The latter extends from a few electron volts above the preedge to about 50 eV higher than the absorption edge and corresponds mainly to multiple-scattering resonances of photoelectrons ejected with low kinetic energy. Apte and Mande (1982) and Belli et al (1980) found that the energy of the main-edge and preedge peaks of manganese oxides varied linearly with the oxidation state of Mn atoms. This positive energy shift with increasing valence results partly from in-

* Present address: Université Joseph Fourier, LGIT, BP 53X, 38041 Grenoble Cedex, France.

0003–004X/92/1112–1133$02.00

creased attraction between the nucleus and the 1s core electrons and partly from the effect of final-state wave functions. Final states of 3d character (preedge region) are more tightly bound and hence are less sensitive to changes in ionicity and in solid-state effects than the more diffuse, higher energy, final states of the main absorption *K* edge (multiple-scattering region). Thus, the oxidation state is more reliably determined from the energy position of the preedge peak than from that of the main absorption edge spectrum. Belli et al. (1980) reported that although molecular orbital (MO) transition assignments are qualitatively correct for interpreting main XANES features, solid-state effects are also important. If confirmed, such spectral sensitivity to the manganese oxide structure would be of particular interest; it would allow Mn*K* XANES to complement EXAFS spectroscopy for the determination of the local structure of hydrous manganese oxides. Fe*K* XANES spectra of minerals have been more extensively studied. Near-edge and main-edge absorption features from Fe*K* XANES spectra have been shown to reflect the site geometry and valence of Fe in minerals (Calas and Petiau, 1983; Waychunas et al., 1983). More recently, Manceau et al. (1990a) applied this spectroscopy to test the possible presence of tetrahedrally coordinated Fe^{3+} in hydrous iron oxides. In this case, Fe*K* preedge features were shown to be particularly sensitive to the $^{[6]}Fe^{3+}/^{[4]}Fe^{3+}$ ratio with a detection limit for $^{[4]}Fe^{3+}$ ions at less than 10 at%. In minerals, Co can be divalent or trivalent, tetrahedrally or octahedrally coordinated, and in a low-spin or high-spin configuration. Facing these contrasting electronic structures, XANES spectroscopy should yield valuable information about the crystal chemistry of Co in hydrous manganese oxides.

Experimental details

Analytical techniques

XANES spectra were obtained at the EXAFS IV station at the LURE synchrotron radiation laboratory (Orsay, France). The electron energy of the DCI storage ring was 1.85 GeV, and the current was between 200 and 250 mA. The incident beam was monochromatized using pairs of reflecting Si (511) crystals so that the Bragg angle near the Mn*K* edge was near 66°. At this angle, the energy spread due to vertical divergence of the beam was 0.45 eV, and the intrinsic width of the reflection curve (Darwin width) equaled 0.05 eV. These widths are significantly smaller than the Mn core-level width (1.16 eV) that results from core hole lifetime. The overall resolution of XANES spectra was equal to the convolution of the instrument with the core-level widths and was as small as 1.2–1.3 eV. With this high level of resolution, experimental spectral broadening was negligible. Harmonics due to higher order reflections were filtered out with borosilicate glass mirrors (Sainctavit et al., 1988). The energy calibration of Mn*K* XANES spectra was made taking a maximum of the preedge peak for $MnCr_2O_4$ at 6538.7 eV. The preabsorption feature in $MnCr_2O_4$ was repeatedly measured to monitor the stability of the energy calibration. Mn and Fe preedge spectra were recorded in steps of 0.06 and 0.13 eV, respectively.

Corrected preedge absorption structure was obtained by subtracting the arc-tangent–fitted interpolated tail of the main edge from the observed spectra. The absorbance was then normalized with respect to the absorption jump of the main edge ($\Delta\mu$). This jump was determined by fitting first-order polynomials to the data 100 eV below the preedge and from 100 to 400 eV above. The difference between these two lines (at the energy at which the preedge starts) was used as the normalization factor for the corrected preedge. The reliability of the experimental measurements and our analytical treatment were confirmed by recording several spectra of the same sample during different beam sessions.

Materials

A series of well-crystallized manganese, iron, and cobalt oxides, which served as reference compounds, and other Mn-, Fe-, and Co-bearing minerals were analyzed. The minerals are listed in Table 1 along with their formulae and selected crystallographic data.

Birnessite. A synthetic birnessite sample, $Na_4Mn_{14}O_{27}\cdot 9H_2O$, synthetized by Giovanoli (Giovanoli et al., 1969, 1970a, 1970b; Giovanoli and Stähli, 1970) was examined, in addition to two natural birnessite samples (B1, M12) from (Fe,Mn) micronodules of the Clarion-Clipperton province, Pacific Ocean (Chukhrov et al., 1978a; Shterenberg et al., 1985). Sample B1 contains Mn (MnO_2 = 67.66 wt%) and, in addition, Mg, K, Na, and Ca (MgO = 8.58 wt%, K_2O = 2.43 wt%, Na_2O = 1.90 wt%, and CaO = 0.52 wt%). A noticeable feature of sample M12 is the absence of Ca, Mg, K, and Na and the presence of small amounts of Ni, Cu, and Co (NiO = 1.65%, CuO = 0.92%, and Co_2O_3 = 0.16%).

Vernadite. A synthetic vernadite sample (δ-MnO_2) was prepared by adding H_2O_2 to a stirred 1 *M* $KMnO_4$ solution at room temperature (Chukhrov et al., 1987). The precipitate was freeze dried, then washed with 0.1 *M* HNO_3, distilled H_2O and finally 1 *M* NaCl. A large collection of Fe-bearing natural vernadite samples previously studied by Chukhrov et al. (1987, 1988) and Manceau and Combes (1988) were examined further. Data from EDS indicated that the Mn/Fe ratio in these natural particles ranged from 3/1 to 1/1.

Mn-bearing goethite. A sample of manganese goethite from the Fe-Mn crusts of Krylov Underwater Mountain (Atlantic Ocean) has been described by Varentsov et al. (1989) as goethite groutite. Our EDS data showed the mean composition of particles to be about 50% MnO_2 and 50% Fe_2O_3, but with a variable MnO_2 content ranging from 33 to 62%.

Asbolane. Three asbolane samples were investigated. Two cobalt nickel asbolane samples from New Caledonia Ni ore deposits were previously studied by Manceau et al. (1987) using EXAFS spectroscopy. A cobalt asbolane sample from Saalfeld (Germany) was originally charac-

Table 1. Selected mineralogical and crystallographic information on samples

Mineral name	Ideal composition	Oxidation state and site occupation of cation	Full point group
	Manganese oxides		
Phyllomanganates			
Buserite (2-D)	MnO_2	$^{[6]}Mn^{4+}$	—(1)
Lithiophorite (2-D)	$(Al,Li)MnO_2(OH)_2$	$^{[6]}Mn^{4+}$	C_{2h}, C_3(2)
Birnessite (2-D)	$Na_4Mn_{14}O_{27}\cdot 9H_2O$	$^{[6]}Mn^{4+}$	C_{2h}(3)
Asbolane (2-D)	$Mn(O,OH)_2(Ni,Co)_x(O,OH)_2\cdot nH_2O$	$^{[6]}Mn^{4+}$	—(4)
Chalcophanite (2-D')	$ZnMn_3O_7\cdot 3H_2O$	$^{[6]}Mn^{4+}$	C_i(5)
Vernadite (2-D')	δ-MnO_2	$^{[6]}Mn^{4+}$	—(6)
Tectomanganates			
Todorokite	$(Na,Ca,K)_{0.3-0.7}(Mn,Mg)_6O_{12}\cdot nH_2O$	$^{[6]}Mn^{4+}$	C_{2h}(7)
Psilomelane (romanachite)	$(Ba,H_2O)_2Mn_5O_{10}$	$^{[6]}Mn^{4+}$	C_{2h}(8)
Hollandite	$(Ba,Na,K)Mn_8(O,OH)_{16}$	$^{[6]}Mn^{4+}$	C_{2h}, C_{4h}(9)
Ramsdellite	α-MnO_2	$^{[6]}Mn^{4+}$	D_{2h}(10)
Pyrolusite	MnO_2	$^{[6]}Mn^{4+}$	D_{4h}(11)
Other			
Rhodochrosite	$MnCO_3$	$^{[6]}Mn^{2+}$	D_{3d}(12)
Manganese spinel	$MnCr_2O_4$	$^{[4]}Mn^{2+}$	O_h(13)
Hausmannite	Mn_3O_4	$^{[6]}Mn^{3+} + {}^{[4]}Mn^{2+}$	O_h(13)
Feitknechtite	β-MnOOH	$^{[6]}Mn^{3+}$	—(14)
	Iron oxides		
Goethite	α-FeOOH	$^{[6]}Fe^{3+}$	D_{2h}(15)
Akaganeite	β-FeOOH	$^{[6]}Fe^{3+}$	D_{2h}(16)
Lepidocrocite	γ-FeOOH	$^{[6]}Fe^{3+}$	D_{2h}(17)
Feroxyhite	δ-FeOOH	$^{[6]}Fe^{3+}$	D_{3d}(18)
Ferrihydrite	$5Fe_2O_3\cdot 9H_2O$	$^{[6]}Fe^{3+}$	—(19)
Hematite	α-Fe_2O_3	$^{[6]}Fe^{3+}$	D_{3d}(20)
Maghemite	γ-Fe_2O_3	$^{[6]}Fe^{3+} + {}^{[4]}Fe^{3+}$	O_h(21)
Iron phosphate	$FePO_4$	$^{[4]}Fe^{3+}$	D_3(22)
	Co compounds		
Erythrite	$Co_3(AsO_4)_2\cdot 8H_2O$	$^{[6]}Co^{2+}$	—(23)
Cobalt spinel	$CoAl_2O_4$	$^{[4]}Co^{2+}$	O_h(13)
Heterogenite	CoOOH	$^{[6]}Co^{3+}$	D_{6h}(24)

Note: 1 = Giovanoli (1980a); 2 = Wadsley (1952), Pauling and Kamb (1982); 3 = Post and Veblen (1990); 4 = Drits (1987); 5 = Wadsley (1953), Post and Appleman (1988); 6 = Chukhrov et al. (1978b), Giovanoli (1980b); 7 = Post and Bish (1988); 8 = Wadsley (1953), Turner and Post (1988); 9 = Byström and Byström (1950), Post et al. (1982), Miura (1986), Vicat et al. (1986); 10 = Byström (1949); 11 = Baur (1976); 12 = Effenberger et al. (1981); 13 = Hill et al. (1979); 14 = Bricker (1965); 15 = Szytula et al. (1968); 16 = Szytula et al. (1970); 17 = Ewing (1935); 18 = Patrat et al. (1983); 19 = Towe and Bradley (1967); 20 = Blake et al. (1966); 21 = Hägg (1935), Verwey (1935); 22 = Arnold (1986); 23 = Taylor and Heiding (1958); 24 = Delaplane et al. (1969), Deliens and Goethals (1973).

terized by Chukhrov et al. (1982a) by X-ray and electron diffraction, EDS and XPS. The cation composition of the last has Mn, Co, and Ca in the ratio 1:0.63:0.12.

Results

Mn*K* preedge

Preedge spectra for some of the reference compounds are presented in Figure 1a. A shift in the preedge toward higher energy occurs with an increase in the oxidation state of Mn in the mineral regardless of the coordination number. Spectra for several manganese oxides are shown in Figure 1b. There is a change in intensity and full-width at half maximum (FWHM) for the preedge peaks that directly reflects progressive changes in structure. As the size of the tunnel of octahedra increases, the preedge intensity and FWHM decrease (compare Fig. 2 with Fig. 1b). This rather unexpected relationship was verified by recording these spectra several times at different beam sessions. Variations were not due to a preferential orientation of the powder in the polarized X-ray beam (i.e., texture effect) as shown by recording spectra of several samples at the "magic angle" (Manceau et al., 1990b). Additionally, comparison of the spectra of two pyrolusite, four todorokite, and two psilomelane samples from different localities showed that the chemistry and origin of the minerals had no influence on spectral shape. We conclude that the intensity and shape of a preedge spectrum depend only on the structure of the manganese oxide mineral and that this information can be used on a phenomenologic basis to assess the local structure of unknown structures. Preedge spectra of unknown samples are compared to those of the reference minerals in Figure 3. The energy of the preedge peak is the same as those in tetravalent manganates, and the intensity is always found to lie between those of buserite and todorokite.

Mn*K* main edge

Main-edge spectra for some of the Mn reference compounds are presented in Figure 4a. The main edge shifts toward higher energy with increasing formal oxidation state of Mn ions. The steeply rising part of the XANES spectra of manganates and hydrous manganese oxides approximately superimposes upon that of pyrolusite (Fig. 4b, 4c). However, the spectral shape and, more specifically, the edge-crest intensity, progressively increase from pyrolusite to buserite. This is opposite to the trend observed for the preedge spectra.

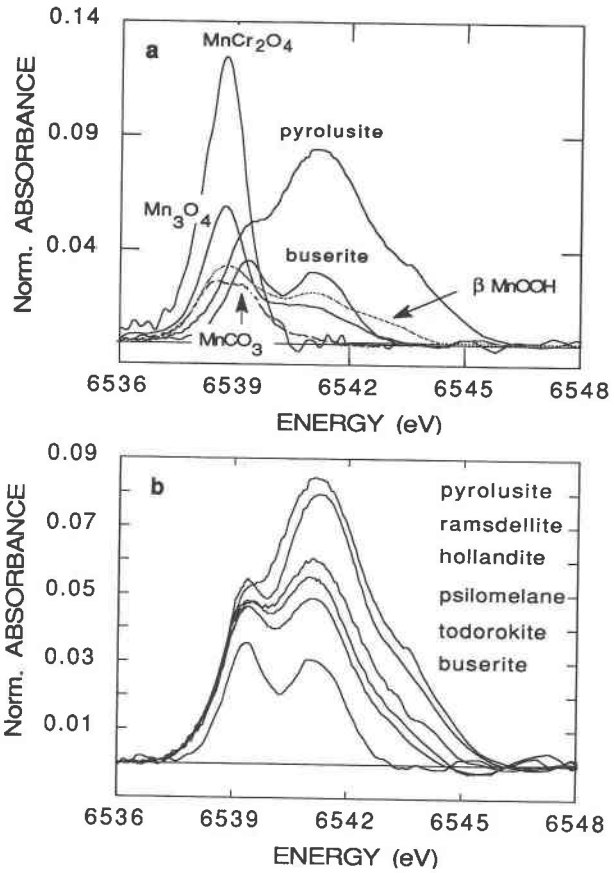

Fig. 1. Mn*K* preedge spectra of reference materials. (**a**) $MnCr_2O_4$ ($^{[4]}Mn^{2+}$), $MnCO_3$ ($^{[6]}Mn^{2+}$), β-MnOOH ($^{[6]}Mn^{3+}$), Mn_3O_4 ($^{[4]}Mn^{2+}$ + $^{[6]}Mn^{3+}$), buserite ($^{[6]}Mn^{4+}$), pyrolusite ($^{[6]}Mn^{4+}$). (**b**) MnO_2 polymorphs. From the bottom: buserite, todorokite, psilomelane, hollandite, ramsdellite, and pyrolusite.

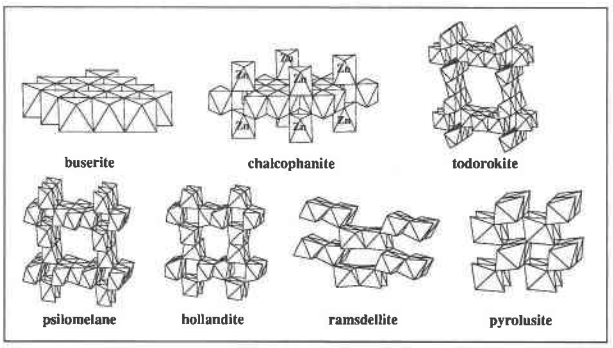

Fig. 2. Schematic structure of MnO_2 polymorphs. Phyllomanganates have no (2-D) or few (2-D′) corner linkages of Mn octahedra. This family includes buserite (2-D), lithiophorite (2-D), asbolane (2-D), chalcophanite (2-D′), and birnessite (2-D or 2-D′). Tectomanganates have many corner linkages and 3-D O framework. They are built of single to multiple chains of edge-sharing Mn octahedra. These chains are cross-linked by corners, resulting in tunnel structures. This family includes todorokite, psilomelane (or romanachite), hollandite, ramsdellite, and pyrolusite.

Fe*K* XANES

The Fe*K* preedge spectra for some $^{[4]}Fe^{3+}$ and $^{[6]}Fe^{3+}$ reference minerals are presented in Figure 5a. Figure 5b and 5c show the spectra of vernadite compared to those for reference minerals and simulated compositions $^{[4]}Fe^{3+}/(^{[6]}Fe^{3+} + {}^{[4]}Fe^{3+})$ using linear combinations of goethite and $FePO_4$ spectra.

Co*K* XANES

The Co*K* main absorption edge spectra from some $^{[6]}Co^{2+}$ (erythrite), $^{[4]}Co^{2+}$ ($CoAl_2O_4$), and $^{[6]}Co^{3+}$ (CoOOH) reference minerals are presented in Figure 6 along with that of the Saalfeld cobalt asbolane. The spectrum of asbolane is featureless and resembles those of erythrite and CoOOH. The main-edge energy for asbolane is the same as that of CoOOH, but it is larger than that of erythrite.

Discussion

Interpretation of spectra from reference compounds

The Mn preedge spectra (Fig. 1) show a chemical shift that relates to the oxidation state of Mn in the mineral. A shift was previously noted by Belli et al. (1980), but our data show a significantly larger shift. This is demonstrated, for example, by the 1.5-eV difference between Mn^{2+} and Mn^{4+} ions in comparison with a few tenths of an electron volt reported by Belli and coworkers. We can speculate that lower spectral resolution in the older experiments has reduced the precision of the determination of preedge energies.

The intensity of the preedge spectrum for $MnCr_2O_4$ is four times greater than that for $MnCO_3$ (Fig. 1a). The data agree with the general observation that in a tetrahedral environment preedge spectra are four to seven times more intense (see, e.g., Lytle et al., 1988). The enhanced intensity can be explained by dipole selection rules, although a weak contribution of quadrupole transitions has been experimentally demonstrated (Dräger et al., 1988; Poumellec et al., 1991). Allowed dipole transitions from the 1s level must have a final wave function with p symmetry. Therefore, a major part of the preedge is usually ascribed to electric dipole transitions to p-like states hybridized with 3d states. The ligand-field induced p-d mixing is symmetry dependent, and Brouder (1990) has recently demonstrated that the transition strength is ruled by the full-point group symmetry of the crystal: it is negligible or intense depending on the centrosymmetry of the full point group. For example, the low preedge intensity of sixfold coordinated Mn^{2+} ions in $MnCO_3$ results from the existence of an inversion center in the D_{3d} full point group (Table 1).

Comparison of the preedge spectra from $MnCr_2O_4$ ($^{[4]}Mn^{2+}$) and $MnCO_3$ ($^{[6]}Mn^{2+}$) shows that for a given oxidation state, the FWHM decreases with a decrease in coordination number. Similarly, comparison of spectra from $MnCO_3$, β-MnOOH ($^{[6]}Mn^{3+}$) and β-MnO_2 ($^{[6]}Mn^{4+}$) indicates that for a fixed coordination number, the preedge FWHM increases with the oxidation state. This increase in line width as coordination changes form four- to six-

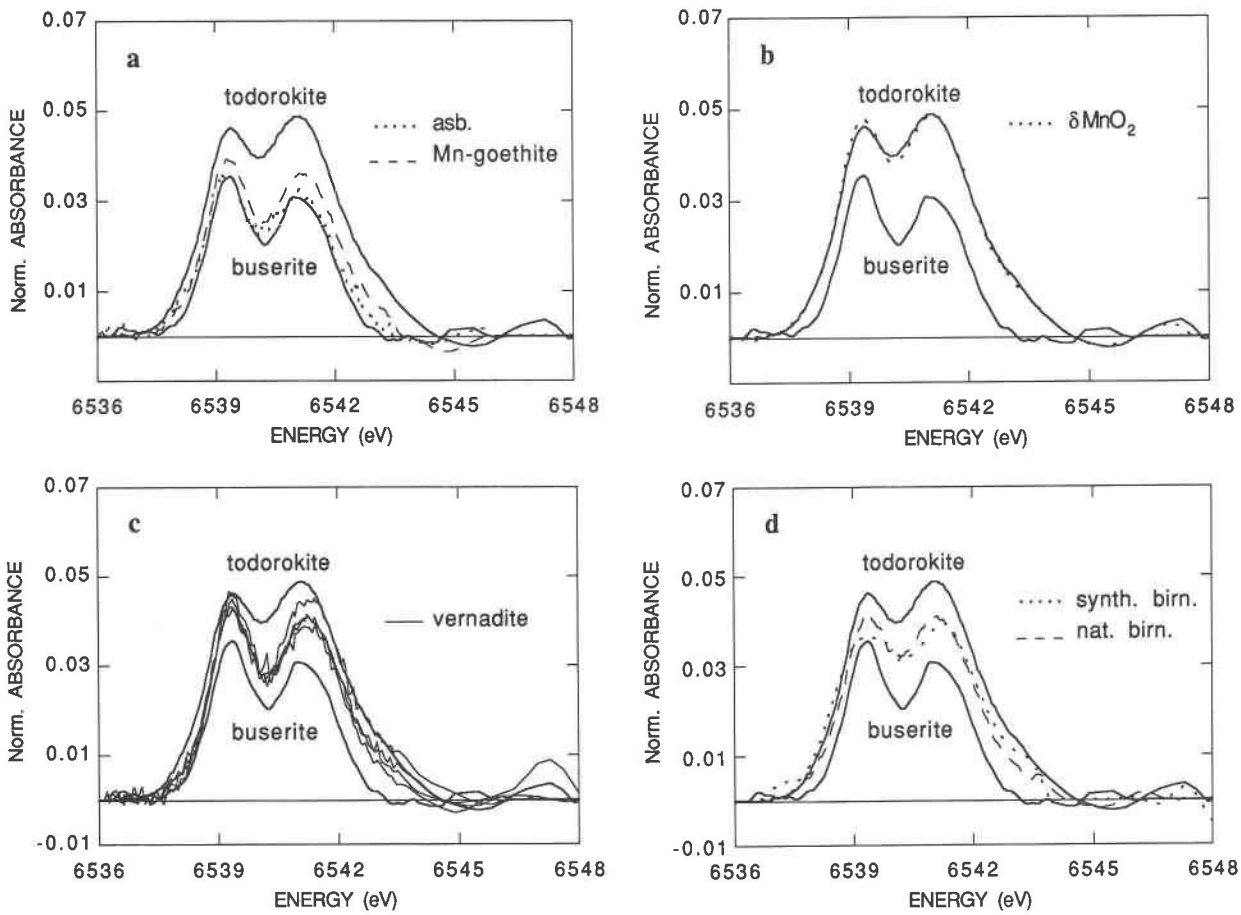

Fig. 3. Mn*K* preedge spectra of samples and reference materials compared with spectra of buserite and todorokite. (**a**) Asbolane from Germany and manganese goethite; (**b**) δ-MnO_2, (**c**) vernadite, (**d**) birnessite.

fold, and from Me^{n+} to $Me^{(n+1)+}$, is consistent with the 1s-3d type of assignment because the line width reflects the ligand field splitting of the 3d orbitals. For example, $^{[6]}Mn^{3+}$ is a Jahn-Teller ion and the splitting of the individual orbital states is large enough that the preedge spectrum of β-MnOOH is separated into two well-resolved absorption bands.

In lepidocrocite, goethite, and akaganeite (Fig. 5a) 1s → 3d absorption is weak, only about 3–4% of the intensity of the absorption jump. The slightly increased intensity of the preedge spectrum of hematite in comparison with those of other $^{[6]}Fe^{3+}$ reference compounds is anomalous, since the space point group of hematite (D_{3d}) and the Fe site symmetry ($\bar{3}m$) are both centrosymmetric. Increased intensity may result from long-range order effects, which are known to influence preedge characteristics (Dräger et al., 1988). In the case of $FePO_4$ ($^{[4]}Fe^{3+}$), a lack of inversion center at the Fe site is reflected by the fivefold higher intensity for the preedge spectrum.

Oxidation state and site occupation of Mn

All of the preedge spectra for hydrous manganese oxides (vernadite, δ-MnO_2, asbolane, birnessite) are found at the same energy as those of manganese oxides (Fig. 3), suggesting that the range of valences for Mn atoms is limited. This interpretation is corroborated by main-edge energy data (Fig. 4b, 4c). The absence of compelling evidence for large amounts of Mn^{3+} and Mn^{2+} in any of these manganese oxides agrees with recent studies. Indeed, even though it has long been assumed that Mn atoms in manganates were divalent and tetravalent, numerous XRD studies (Post et al., 1982; Giovanoli, 1985; Tamada and Yamamoto, 1986; Vicat et al., 1986; Post and Bish, 1988; Post and Appleman, 1988), XPS studies (Murray and Dillard, 1979; Chukhrov et al., 1982b; Dillard et al., 1982), and redox titration studies (Murray et al., 1984) have demonstrated that they are not. The scarcity of low-valence Mn ions is consistent with the structure of nearly all tectomanganates and phyllomanganates, where the unit-cell parameters of the plane of the octahedral chains, ribbons, and layers are similar. Indeed, if manganese oxides contained abundant divalent or trivalent Mn atoms, these heterovalent cations would lead to significant variations in the unit-cell parameters.

The proportion of Mn^{3+} may vary from one structure and one sample to another, but the studies cited above suggest that it generally constitutes less than about 20%. Given the relatively weak chemical shift between Mn^{3+}

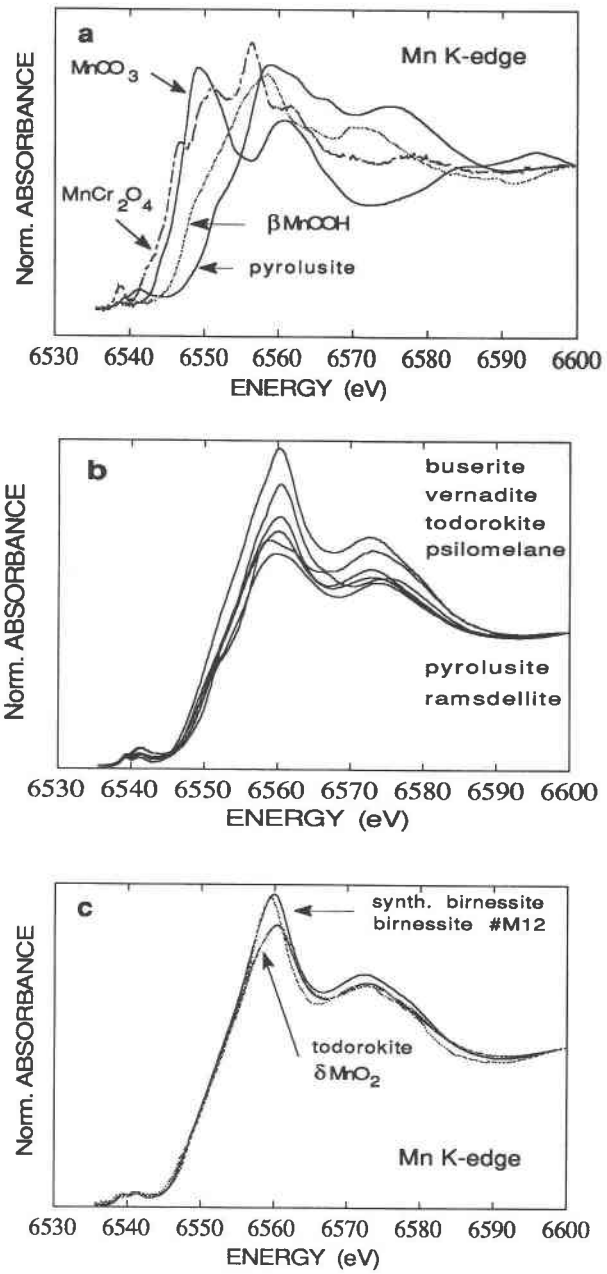

Fig. 4. Mn*K* main edges of manganese oxides. (**a**) Reference compounds: $MnCO_3$ ($^{[6]}Mn^{2+}$), $MnCr_2O_4$ ($^{[4]}Mn^{2+}$), β-MnOOH ($^{[6]}Mn^{3+}$), pyrolusite ($^{[6]}Mn^{4+}$). (**b**) Evolution of the shape of the 1s → 4p transition in the tectomanganate-phyllomanganate series. (**c**) Comparison of δ-MnO_2 spectrum to those of todorokite and birnessite. Note similarity of δ-MnO_2 and todorokite spectra.

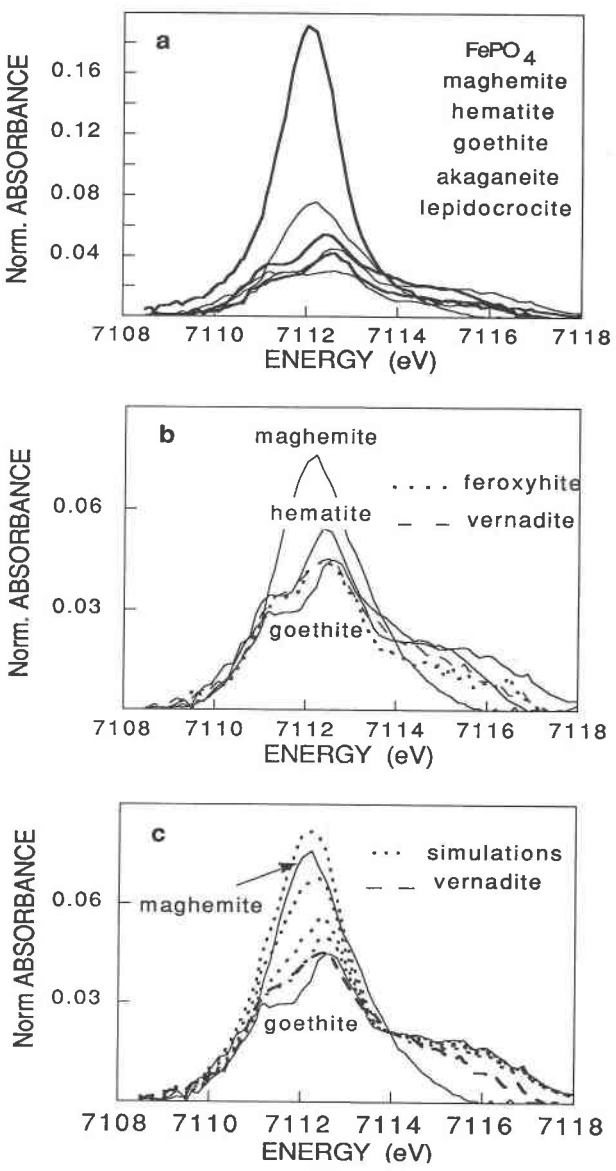

Fig. 5. Fe*K* preedge spectra. (**a**) Reference minerals. From lowest intensity to highest: lepidocrocite, akaganeite, goethite, hematite, maghemite ($^{[6]}Fe^{3+}$ + $^{[4]}Fe^{3+}$), and $FePO_4$ ($^{[4]}Fe^{3+}$). (**b**) Vernadite spectrum compared with selected reference spectra. (**c**) Dotted lines represent linear combinations of goethite and $FePO_4$ spectra. From lowest intensity to highest: 5% $^{[4]}Fe^{3+}$, 10% $^{[4]}Fe^{3+}$, 20% $^{[4]}Fe^{3+}$, and 30% $^{[4]}Fe^{3+}$.

and Mn^{4+} preedge spectra and the high variability of their intensities among tetravalent manganates, our precision is within this range. We successfully fitted the experimental spectrum for Mn_3O_4 spinel with a weighted sum of two spectra: $\frac{1}{3}MnCr_2O_4$ ($^{[4]}Mn^{2+}$) and $\frac{2}{3}\beta$-MnOOH ($^{[6]}Mn^{3+}$) (Fig. 7c). On the basis of this result, we have estimated the detection limit of $^{[4]}Mn^{2+}$ ions by XANES to be about 10 at%.

Mn atoms in manganese goethite are also in a tetravalent state (Fig. 3a). This is not surprising because Mn minerals, associated with iron oxyhydroxides in the oxidized zone of weathering profiles or on the sea floor, are exclusively Mn^{4+} oxides. Based on an analogy with the large site distortion of Cu^{2+} (Jahn-Teller ion) in copper magnesium phyllosilicates (Decarreau, 1985; Decarreau et al., 1992), Mn^{3+} would be unlikely to enter the goethite

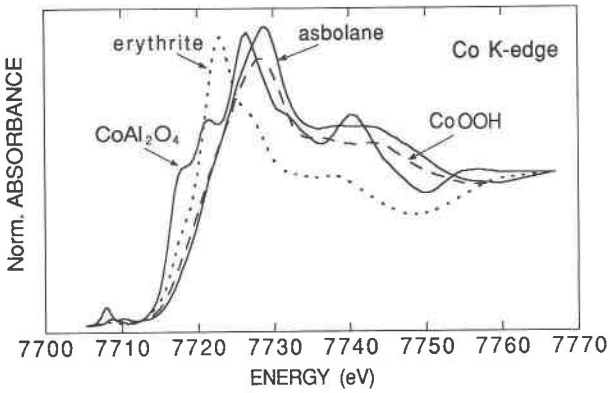

Fig. 6. Co*K* main edge spectra of reference minerals. Erythrite ($^{[6]}Co^{2+}$), $CoAl_2O_4$ ($^{[4]}Co^{2+}$), CoOOH ($^{[6]}Co^{3+}$) compared with the spectrum of Co in asbolane. The amplitude was calibrated by assuming the atomic part of the absorption jump as a normalization value.

structure in large amounts, thus limiting the extent of the goethite-groutite solid solution. This explanation may equally apply to the experiments of Stiers and Schwertmann (1985) and Ebinger and Schulze (1989), who found that the proportion of Mn^{3+} substituted for Fe in goethite was less than 10 at% and 14–34 at%, respectively.

Local structure of hydrous manganese oxides

Within the phyllomanganate-tectomanganate series, there is a progressive change in the intensity and the shape of preedge and main-edge spectra (Figs. 1b, 4b). Interpretation of the trend is not straightforward and will be considered, with some details, below.

Preedge. One possibility is that an increase in peak intensity (from buserite to pyrolusite) correlates with an increase in the Mn^{4+}/Mn^{3+} ratio. In order to test this hypothesis, linear combinations of pyrolusite and β-MnOOH spectra were computed (Fig. 7a). Although the shape and intensity of this suite of theoretical spectra reproduce the trends observed in the tectomanganate-phyllomanganate series (Fig. 1), the simulations shift progressively to lower energy as Mn^{3+} increases. The opposite situation is experimentally observed in reference minerals and samples: the lower the amplitude, the higher the energy of the left side of the preedge of manganates (Figs. 1b, 3). Thus, the preedge spectra of MnO_2 polymorphs cannot be fitted by a linear combination of Mn^{4+}-Mn^{3+} reference spectra.

A second interpretation might be attempted using symmetry effects. However, all of the manganese oxides are centrosymmetric (Table 1), which theoretically precludes any intensity for the forbidden 1s → 3d preedge absorption. Thus, it is concluded that the preedge trend among tetravalent manganates cannot be qualitatively interpreted within a simple quantum molecular-orbital framework.

A third possibility might explain the trend in terms of changes in average Mn-O bond distances. In V compounds (Wong et al., 1984) and in some transition metal

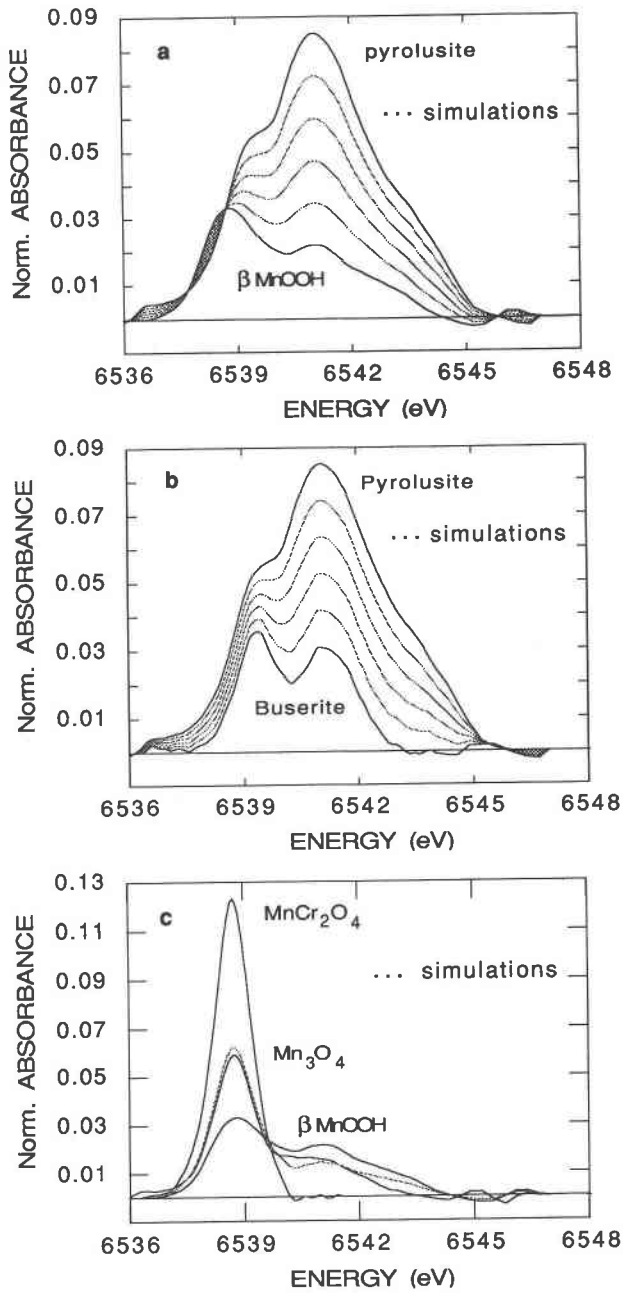

Fig. 7. Simulations of preedge spectra. (**a**) Linear combinations of β-MnOOH and pyrolusite. From lowest intensity to highest: 80, 60, 40, and 20% Mn^{3+}. (**b**) Linear combinations of buserite and pyrolusite. From lowest intensity to highest: 80, 60, 40, and 20% of buserite. (**c**) Dotted line: comparison of simulated Mn_3O_4 spectrum assuming $\frac{1}{3}{}^{[4]}Mn^{2+}$ ($MnCr_2O_4$) and $\frac{2}{3}{}^{[6]}Mn^{3+}$ (β-MnOOH) with selected references.

complexes (Kutzler et al., 1980), variations in the oscillator strength of the preedge were attributed to a decrease in size of the coordination polyhedron. This empirical relationship between the size of the molecular cage, defined by the nearest-neighbor ligands, and preedge intensity was interpreted within a quantum-mechanical frame-

work (Kutzler et al., 1980; Wong et al., 1984). From that, it was deduced that the smaller the cage, the higher the intensity of the 1s → 3d transition. Mean Mn-O bond length is at a minimum in pyrolusite (1.89 Å; Baur, 1976) and increases progressively through chalcophanite-todorokite (1.91 Å; Post and Appleman, 1988; Post and Bish, 1988), hollandite (1.92 Å; Vicat et al., 1986; Miura, 1986), psilomelane (1.93 Å; Wadsley, 1953), and lithiophorite and birnessite (1.94 Å; Post and Appleman, 1988; Post and Veblen, 1990). However, in all likelihood, bond-length variation is not large enough to account completely for the threefold increase in the intensity of the pyrolusite spectrum relative to that of buserite. In our opinion, it should rather be regarded as a factor that may reinforce some other unelucidated effect.

Although we are unable to provide an explanation based on physical parameters for the trends within the manganate suite, we can state that peak intensity is roughly proportional to the ratio of edge- to corner-sharing MnO_6 octahedra, i.e., the larger the tunnel size (Turner and Buseck, 1979), the lower the peak intensity and the smaller its width. The lowest magnitude is observed for sodium buserite, which has no corner-sharing octahedra (details presented in Manceau et al., 1992), and the highest intensity is obtained for pyrolusite, where each octahedron shares eight corners and two edges. Our structural interpretation is strengthened by the fact that the trend observed in the phyllomanganate to tectomanganate series can be reproduced by linear combinations of buserite and pyrolusite spectra (Figs. 1b, 7b). Furthermore, the importance of long-range order effects on preedge features has a parallel in the case of hematite (Dräger et al., 1988). Thus, preedge intensity offers a clue to local structure of unknown manganates.

The preedge spectra of hydrous manganese oxides can be divided into three groups based on their height (Fig. 3). The first group includes samples that have a weak preedge peak, such as the asbolanes from Saalfeld and New Caledonia and the manganese goethite. Their spectra show no evidence of vertex-sharing MnO_6 octahedra (Fig. 3a). The second group contains δ-MnO_2. The similarity of this spectrum with that of todorokite (Fig. 3b) suggests that δ-MnO_2 does not possess a layered structure. This interpretation is fully consistent with main-edge spectra and data from EXAFS and XRD and indicates a 3-D O framework structure (Manceau et al., 1992). The third group comprises natural vernadite and birnessite. These spectra are of intermediate height, ranging between those of the two preceding groups of samples, which suggests that vernadite and birnessite might have some corner-sharing octahedra in their structure.

Main edge. The shape and intensity of the main-edge crest of tetravalent manganates progressively change in the series from pyrolusite-ramsdellite to buserite (Fig. 4b). Spectral features observed on the main absorption edge are usually interpreted using molecular orbital theory, sometimes in terms of density of states, or by multiple scatterings about the atomic cage constituted by nearest coordination shells (see, e.g., the review of Petiau et al., 1987). In the first of these theoretical approaches, the main absorption maximum is identified as a dipole 1s → 4p transition to the triply degenerate $4t_{1u}$ molecular orbital (Apte and Mande, 1980). Hence, splittings or broadening in the vicinity of the edge crest is evidence of broken degeneracy in the antibonding orbitals due to asymmetric metal-ligand bonding. The symmetry of final states can be probed by angular measurements (Hahn and Hodgson, 1983; Frétigny et al., 1986) using single crystals, but in their absence, near main-edge spectral features are mainly interpreted qualitatively, by comparing known with unknown structures.

The main-edge spectrum of $MnCO_3$ is featureless, with a single, well-defined crest (Fig. 4a). This edge shape agrees with the high symmetry of the Mn site ($\bar{3}m$), with the full point group (D_{3d}), and with six equivalent Mn-O distances (2.19 Å). The main-edge spectra of phyllomanganates are also featureless (Fig. 4b), indicating a highly symmetric Mn site. This interpretation corroborates that determined from their weak preedge intensity. In contrast, several features are observed on the edge crests of pyrolusite ($^{[6]}Mn^{4+}$) and β-MnOOH, which, in the case of $^{[6]}Mn^{3+}$ ions, can be interpreted by the nondegeneracy of p orbitals as a result of Jahn-Teller distortion. In pyrolusite, p orbitals are also nondegenerate, since the Mn octahedron is stretched along the **z** axis [d(Mn-O) = 1.88 Å × 4; d(Mn-O) = 1.90 Å × 2, site symmetry *mmm*; Baur, 1976]. Although main-edge features are sensitive to subtle changes in site geometry (Waychunas, 1987); it is surprising that this small variation in the Mn-O distances leads to such large crest broadening. Apparently, a simple molecular orbital approach is not sufficient to describe the edge features of manganese oxides; it is necessary to consider a larger molecular cluster that would include nearest cation shells.

Solid-state effects in the main-edge spectra of manganese oxides were first recognized by Belli et al. (1980). They interpreted spectral differences between MnO and β-MnO_2 (pyrolusite) in terms of differences in octahedral linkages: each octahedron shares 12 edges in the former oxide and two edges and eight corners in the latter. Of particular interest is the similarity of spectra for MnO and the phyllomanganates: all are characterized by an intense and featureless 1s → 4p transition indicating a completely unfilled final p state. These similarities in spectra reinforce the idea that in manganese oxides nearest cation shells are important for the final state wave function, as in both of these structures MnO_6 octahedra are linked only by edges. However, the most convincing support for the existence of solid-state effects in the vicinity of the edge crest comes from a comparison of spectra from TiO_2 (Waychunas, 1987) and MnO_2. Rutile and pyrolusite, which are isostructural, possess similar spectra. The same is true for phyllomanganates and anatase, where chains of edge-shared TiO_2 octahedra are linked through edges yielding a pseudolayered structure.

The edge crest increases in intensity and is less broad

from tectomanganates to phyllomanganates (Fig. 4b). On the basis of the preceding discussion, this trend may also be explained with a solid-state approach. A progressive change in local structure is manifested by an increase in the number of edge-sharing octahedra at the expense of corner-sharing octahedra. Thus, short-range mineral structure can be deduced from main-edge spectra, just as from preedge spectra. Edge-crest spectral features provide information about the way octahedra are linked to each other, so their analysis often reinforces evidence derived from preedge data.

The similarity between the main-edge spectra of todorokite and δ-MnO_2 affords an additional clue to the structural difference between birnessite and δ-MnO_2 (Fig. 4c). The Mn*K* edges of vernadite (Fig. 4b) and birnessite (Fig. 4c) are all similar to those of reference phyllomanganates. They have a single, well-defined, and intense edge crest suggesting similar short-range order. This finding appears at variance with preedge results, which suggested a scarcity of corner-sharing octahedra in both vernadite and birnessite. Given the evident low sensitivity of XANES spectroscopy to short-range structure, one may conclude that both preedge and main-edge results are convergent, indicating that, if present, there are few Mn-O-Mn vertex linkages, or they are at least less abundant than in todorokite.

Site occupation of Fe

Fe^{3+} ions, unlike Mn^{4+}, can occupy both sixfold- and fourfold-coordinated sites in minerals. The low crystallinity of ferric gels results in a large distribution of Fe^{3+} sites that have slightly different types and arrangements of neighboring ions. This local disorder renders classical structural and spectroscopic methods, such as Mössbauer spectroscopy (Murad and Schwertmann, 1980; Cardile, 1988), essentially insensitive to the coordination environment of Fe. Fortunately, this is not a limitation for preedge spectroscopy: it has been successfully used to determine the Fe sites in natural and synthetic hydrous ferric gels (Combes et al., 1989, 1990; Manceau et al., 1990a).

Preedge spectra of all vernadite samples are similar to that of feroxyhite (Fig. 5b), whose structure is similar to that of hematite (Patrat et al., 1983). Thus, we do not detect fourfold-coordinated Fe in vernadite. The ability of preedge spectroscopy to detect the presence of $^{[4]}Fe^{3+}$ can be evaluated from the examination of the maghemite (γ-Fe_2O_3) spectrum. If we compare the full 1s $\rightarrow$ 3d intensity of maghemite to a linear combination of spectra for goethite and $FePO_4$, a mean $^{[4]}Fe^{3+}$ concentration of 27% is determined (Fig. 5c). This estimate can be compared with structural data from the literature to assess the site occupancy of Fe in an unknown oxyhydroxide. The γ-Fe_2O_3 possesses a defect spinel structure, and there has been some controversy over the distribution of vacancies (see, e.g., Sinha and Sinha, 1957; Ferguson and Hass, 1958; Annersten and Hafner, 1973). Depending on the author and probably on the nature of the material studied, the distribution of vacancies ranges from a statistical distribution over all tetrahedral and octahedral cation sites to a position exclusively at octahedral lattice sites. The percentage of $^{[4]}Fe$ may be considered to be between 33 and 37%, which is significantly greater than our experimental value (27%). In the worst case, our determination of the tetrahedral content derived from the preedge spectroscopy might be underestimated by 10%. Based on the similarity of vernadite to feroxyhite spectra and this 10% detection limit, we conclude that there is no evidence for fourfold-coordinated Fe^{3+} ions in vernadite.

Electronic structure of Co in asbolane

The main-edge structure and energy suggest sixfold coordination and a trivalent state for Co in asbolane. This interpretation agrees with the Co-(O,OH) distance determined from our EXAFS data. This topic will be discussed further after presentation of more data in the second part of this work (Manceau et al., 1992).

Conclusions

This study demonstrates the potential for XANES spectroscopy in studies of crystal chemical properties of Mn, Fe, and Co in minerals. Specifically, Mn*K* preedge spectra have been shown to reflect changes in the valence and coordination number of Mn atoms. Sensitivity is high enough to allow differentiation of Mn ions with different oxidation states and site occupations as, for instance, the two oxidation states of Mn^{2+} and Mn^{3+} in Mn_3O_4, or the two Mn sites ($^{[4]}Mn$, $^{[6]}Mn$) in γ-Mn_2O_3. Such distinction is not currently possible with other spectroscopic techniques, such as X-ray photoelectron spectroscopy (XPS; Oku et al., 1975; Murray and Dillard, 1979; Dillard et al., 1982; Crowther et al., 1983; Murray et al., 1985), energy electron loss spectroscopy (EELS; Rask et al., 1987), and UV-visible reflectance spectroscopy (Strobel et al., 1987). Preedge spectra have also been shown to be sensitive to the local structure of tetravalent manganese oxides because the intensity MnO_2 spectra depends on the ratio of edge- to corner-sharing MnO_6 octahedra. Thus Mn*K* XANES spectroscopy serves as a structural tool to complement other techniques for studying short-range structure of highly disordered manganese oxides.

The analysis of various hydrous oxides has shown that Mn is essentially tetravalent even in natural Mn-bearing goethite. The detection limit of low-valence Mn ions is estimated to be about 20%. In hydrous manganese oxides, Fe and Co are both trivalent and octahedrally coordinated. The detection limit of $^{[4]}Fe^{3+}$ by Fe*K* preedge spectroscopy is about 10%. The preedge and main-edge spectra of δ-MnO_2 are similar to those of todorokite, indicating that the two structures have a similar ratio of edge- over corner-sharing octahedra. Our evidence contradicts the generally accepted belief that δ-MnO_2 possesses a layered, birnessite-like structure. Additional proof of the distinct structure of δ-MnO_2 and birnessite will be provided through EXAFS and XRD data presented in the second part of this work (Manceau et al., 1992).

Acknowledgments

The authors thank R. Giovanoli for providing the synthetic birnessite sample, D. Bish for providing several hollandite, psilomelane, and todorokite samples, and the staff of the LURE synchrotron radiation facility. A critical reading of a preliminary version by G.A. Waychunas is acknowledged. Last, and not least, the authors express their gratitude to Susan Stipp, who improved the English. This research was supported by CNRS/INSU through the DBT program, grant 90 DBT 1.03 (contribution no. 413).

References cited

Annersten, H., and Hafner, S.S. (1973) Vacancy distribution in synthetic spinels of the series Fe_3O_4-γFe_2O_3. Zeitschrift für Kristallographie, 137, 321–340.

Apte, M.Y., and Mande, C. (1980) The shape and extended fine structure of the manganese K X-ray absorption discontinuity in its oxides. Journal of Physics and Chemistry of Solids, 41, 307–312.

——— (1982) Chemical effects on the main peak in the K absorption spectrum of manganese in some compounds. Journal of Physics C: Solid State Physics, 15, 607–613.

Arnold, H. (1986) Crystal structure of $FePO_4$ at 294 and 20 K. Zeitschrift für Kristallographie, 177, 139–142.

Baur, W.H. (1976) Rutile-type compounds. V. Refinements of MnO_2 and MgF_2. Acta Crystallographica, B32, 2200–2204.

Belli, M., Scafati, A., Bianconi, A., Mobilio, S., Palladino, L., Reale, A., and Burattini, E. (1980) X-ray absorption near edge structures (XANES) in simple and complex Mn compounds. Solid State Communications, 35, 355–361.

Blake, R.L., Hessevick, R.E., Zoltai, T., and Finger, L.W. (1966) Refinement of the hematite structure. American Mineralogist, 51, 123–129.

Bricker, O. (1965) Some stability relations in the system Mn-O_2-H_2O at 25° and one atmosphere total pressure. American Mineralogist, 50, 1296–1354.

Brouder, C. (1990) Angular dependence of X-ray absorption spectra. Journal of Physics and Condensed Matter, 2, 701–738.

Brown, G.E., Jr., Calas, G., Waychunas, G.A., and Petiau, J. (1988) X-ray absorption spectroscopy: Applications in mineralogy and geochemistry. In Mineralogical Society of America Reviews in Mineralogy, 18, 431–512.

Byström, A., and Byström, A.M. (1950) The crystal structure of hollandite, the related manganese oxide minerals, and αMnO_2. Acta Crystallographica, 3, 146–154.

Byström, A.M. (1949) The crystal structure of ramsdellite, an orthorhombic modification of MnO_2. Acta Chemica Scandinavica, 3, 163–173.

Calas, G., and Petiau, J. (1983) Coordination of iron in oxide glasses through high resolution K-edge spectra: Information from the pre-edge. Solid State Communications, 48, 625–629.

Cardile, C.M. (1988) Tetrahedral Fe^{3+} in ferrihydrite: ^{57}Fe Mössbauer spectroscopic evidence. Clays and Clay Minerals, 36, 537–539.

Chukhrov, F.V., Gorshkov, A.I., Rudnitskaya, E.S., and Sivtsov, A.V. (1978a) Birnessite characterization. Izvestia Akademie Nauk, SSSR, Seriya Geologicheskaya, 9, 67–76.

Chukhrov, F.V., Gorshkov, A.I., and Rudnitskaya, E.S. (1978b) On vernadite. Izvestia Akademie Nauk, SSSR, Seriya Geologicheskaya, 6, 5–19.

Chukhrov, F.V., Gorshkov, A.I., Drits, V.A., and Sivzev, A.V. (1982a) New structural varieties of asbolane. Izvestia Akademie Nauk, SSSR, Seriya Geologicheskaya, 6, 69–77.

Chukhrov, F.V., Gorshkov, A.I., Sivtsov, A.V., Dikov, Yu.P., and Berezovskaya, V.V. (1982b) A natural analog of ϵ-MnO_2. Izvestia Akademie Nauk, SSSR, Seriya Geologicheskaya, 56–65. (Translation in International Geology Review, 1983, 708–718.)

Chukhrov, F.V., Drits, V.A., Gorshkov, A.I., Sakharov, B.A., and Dikov, Y.P. (1987) Structural models of vernadites. Izvestia Academie Nauk, SSSR, Seriya Geologicheskaya, 12, 198–204.

Chukhrov, F.V., Manceau, A., Sakharov, B.A., Combes, J.-M., Gorshkov, A.I., Salyn, A.L., and Drits, V.A. (1988) Crystal chemistry of oceanic Fe-vernadites. Mineralogicheskii Zhurnal, 10, 78–92.

Combes, J.-M., Manceau, A., Calas, G., and Bottero, J.-Y. (1989) Formation of ferric oxides from aqueous solutions: A polyhedral approach by X-ray absorption spectroscopy. I. Hydrolysis and formation of ferric gels. Geochimica et Cosmochimica Acta, 53, 583–594.

Combes, J.-M., Manceau, A., and Calas, G. (1990) Formation of ferric oxides from aqueous solutions: A polyhedral approach by X-ray absorption spectroscopy. II. Hematite formation from ferric gels. Geochimica et Cosmochimica Acta, 54, 1083–1091.

Crowther, D.L., Dillard, J.G., and Murray, J.W. (1983) The mechanism of Co(II) oxidation on synthetic birnessite. Geochimica et Cosmochimica Acta, 47, 1399–1403.

Decarreau, A. (1985) Partitioning of divalent transition elements between octahedral sheets of trioctahedral smectites and water. Geochimica et Cosmochimica Acta, 49, 1537–1544.

Decarreau, A., Grauby, O., and Petit, S. (1992) The actual nature of octahedral solid solutions in clay minerals: Results from clay synthesis. Applied Clay Science, in press.

Delaplane, R.G., Ibers, J., Ferraro, J.R., and Rush, J.J. (1969) Diffraction and spectroscopic studies of the cobaltic acid system $HCoO_2$-$DCoO_2$. Journal of Chemical Physics, 50, 1920–1927.

Deliens, M., and Goethals, H. (1973) Polytypism of heterogenite. Mineralogical Magazine, 39, 152–157.

Dillard, J.G., Crowther, D.L., and Murray, J.W. (1982) The oxidation states of cobalt and selected metals in Pacific ferromanganese nodules. Geochimica et Cosmochimica Acta, 46, 755–759.

Dräger, G., Frahm, R., Materlik, G., and Brümmer, O. (1988) On the multipole character of the X-ray transitions in the pre-edge structure of Fe K absorption spectra. Physica Status Solidi B, 146, 287–294.

Drits, V.A. (1987) Electron diffraction and high-resolution electron microscopy of mineral structures. Springer-Verlag, Berlin.

Ebinger, M.H., and Schulze, D.G. (1989) Mn-substituted goethite and Fe-substituted groutite synthesized at acid pH. Clays and Clay Minerals, 37, 151–156.

Effenberger, H., Mereiter, K., and Zemann, J. (1981) Crystal structure refinements of magnesite, calcite, rhodochrosite, siderite, smithonite, and dolomite, with discussion of some aspects of the stereochemistry of calcite type carbonates. Zeitschrift für Kristallographie, 156, 233–243.

Eggleton, R.A., and Fitzpatrick, R.W. (1988) New data and a revised structural model for ferrihydrite. Clays and Clay Minerals, 36, 111–124.

Ewing, F.J. (1935) The crystal structure of lepidocrocite, γ-FeOOH. Journal of Chemical Physics, 3, 420–427.

Ferguson, G.A., Jr., and Hass, M. (1958) Magnetic structure and vacancy distribution in γ-Fe_2O_3 by neutron diffraction. Physical Review, 112, 1130–1131.

Frétigny, C., Bonnin, D., and Cortès, R. (1986) Polarization effects in XANES of layered materials: Alkali-graphite intercalation compounds study. Journal de Physique, C8, 47, 869–873.

Giovanoli, R. (1980a) On natural and synthetic manganese nodules. In I.M. Varentsov and G. Grasselly, Eds., Geology and geochemistry of manganese, vol. 1, p. 159–202. Schweizerbart'sche Verlagsbuchhandlung, Stuttgart.

——— (1980b) Vernadite is random-stacked birnessite. Mineralium Deposita, 15, 251–253.

——— (1985) A review of the todorokite-buserite problem: Implications to the mineralogy of marine manganese nodules: Discussion. American Mineralogist, 70, 202–204.

Giovanoli, R., And Stähli, E. (1970) Oxide und Oxidhydroxide des drei- und vierwertigen Mangans. Chimia, 24, 49–61.

Giovanoli, R., Stähli, E., and Feitknecht, W. (1969) Über Struktur und Reaktivität von Mangan (IV) Oxiden. Chimia, 23, 264–266.

——— (1970a) Über Oxyhydroxide des vierwertigen Mangans mit Schichtengitter, 1. Natrium Mangan (II, III)-Manganat (IV). Helvetica Chimica Acta, 53, 209–220.

——— (1970b) Über Oxidhydroxide des vierwertigen Mangans mit Schichtengitter. 2. Mangan (III)-Manganat (IV). Helvetica Chimica Acta, 53, 453–464.

Hägg, G. (1935) Die Kristallstruktur des magnetischen Ferrioxids, γ-Fe_2O_3. Zeitschrift für physikalische Chemie, B29, 95–103.

Hahn, J.E., and Hodgson, K.O. (1983) Polarized X-ray absorption spectroscopy. In M.H. Chisholm, Ed., Inorganics chemistry: Towards the 21st century. ACS Symposium Series, 211, 431–444.

Harrison, P.M., Fischbach, F.A., Hoy, T.G., and Haggis, G.M. (1967) Ferric oxyhydroxide core of ferritin. Nature, 216, 1188–1190.

Hill, R.J., Craig, J.R., and Gibbs, G.V. (1979) Systematics of the spinel structure type. Physics and Chemistry of Minerals, 4, 317–339.

Kutzler, F.W., Natoli, C.R., Misemer, D.K., Doniach, S., and Hodgson, K.O. (1980) Use of one-electron theory for the interpretation of near edge structure in K-shell X-ray absorption spectra of transition metal complexes. Journal of Chemical Physics, 73, 3274–3288.

Lytle, F.W., Greegor, R. B., and Panson, A.J. (1988) Discussion of X-ray absorption near edge structure: Application to Cu in high T_c superconductors, $La_{1.8}Sr_{.2}CuO_4$ and $YBa_2Cu_3O_7$. Physical Review, B37, 1550–1562.

Manceau, A., and Combes, J.-M. (1988) Structure of Mn and Fe oxides and oxyhydroxides: A topological approach by EXAFS. Physics and Chemistry of Minerals, 15(3), 283–295.

Manceau, A., Llorca, S., and Calas, G. (1987) Crystal chemistry of cobalt and nickel in lithiophorite and asbolane from New Caledonia. Geochimica et Cosmochimica Acta, 51, 105–113.

Manceau, A., Combes, J.-M., and Calas, G. (1990a) New data and a revised model for ferrihydrite: A comment on a paper by R.A. Eggleton and R.W. Fitzpatrick. Clays and Clay Minerals, 38, 331–334.

Manceau, A., Sanz, J., Stone, W.E.E., and Bonnin, D. (1990b) Distribution of Fe in the octahedral sheet of trioctahedral micas by polarized EXAFS. Comparison with NMR results. Physics and Chemistry of Minerals, 17, 363–370.

Manceau, A., Gorshkov, A.I., and Drits, V. (1992) Structural chemistry of Mn, Fe, Co, and Ni in manganese hydrous oxides: Part II. Information from EXAFS spectroscopy and electron and X-ray diffraction. American Mineralogist, 77, 1144–1157.

Miura, H. (1986) The crystal structure of hollandite. Mineralogical Journal, 13, 119–129.

Murad, E., and Schwertmann, U. (1980) The Mössbauer spectrum of ferrihydrite and its relations to those of other iron oxides. American Mineralogist, 65, 1044–1049.

Murray, J.W., and Dillard, J.G. (1979) The oxidation of cobalt(II) adsorbed on manganese dioxide. Geochimica et Cosmochimica Acta, 43, 781–787.

Murray, J.W., Balistrieri, L. S., and Paul, B. (1984) The oxidation state of manganese in marine sediments and ferromanganese nodules. Geochimica et Cosmochimica Acta, 48, 1237–1247.

Murray, J.W., Dillard, J.G., Giovanoli, R., Moers, H., and Stumm, W. (1985) Oxidation of Mn(II): Initial mineralogy, oxidation state and ageing. Geochimica et Cosmochimica Acta, 49, 463–470.

Oku, M., Hirokawa, K., and Ikeda, S. (1975) X-ray photoelectron spectroscopy of manganese-oxygen systems. Journal of Electron Spectroscopy and Related Phenomena, 7, 465–473.

Patrat, G., De Bergevin, F,. Perret, M., and Joubert, J.C. (1983) Structure locale de δ FeOOH. Acta Crystallographica, B39, 165–170.

Pauling, L., and Kamb, B. (1982) The crystal structure of lithiophorite. American Mineralogist, 67, 817–821.

Petiau, J., Calas, G., and Sainctavit, P. (1987) Recent developments in the experimental studies of XANES. Journal de Physique, C9, 48, 1085–1096.

Post, J.E., and Appleman, D.E. (1988) Chalcophanite, $ZnMn_3O_7 \cdot 3H_2O$: New crystal-structure determination. American Mineralogist, 73, 1401–1404.

Post, J.E., and Bish, D.L. (1988) Rietveld refinement of the todorokite structure. American Mineralogist, 73, 861–869.

Post, J.E., and Veblen, D.R. (1990) Crystal structure determinations of synthetic sodium, magnesium, and potassium birnessite using TEM and the Rietveld method. American Mineralogist, 75, 477–489.

Post, J.E., Dreele, R. B., and Buseck, P.R. (1982) Symmetry and cation displacements in hollandites: Structure refinements of hollandite, cryptomelane and priderite. Acta Crystallographica, B38, 1056–1065.

Poumellec, B., Cortes, R., Tourillon, G., and Berthon, J. (1991) Agular dependence of the Ti K edge in rutile TiO_2. Physica Status Solidi B, 164, 319–326.

Rask, J.H., Miner, B.A., and Buseck, P.R. (1987) Determination of manganese oxidation in solids by electron energy-loss spectroscopy. Ultramicroscopy, 21, 321–326.

Sainctavit, P., Petiau, J., Manceau, A., Rivallant, R., Belakhovsky, M., and Renaud, G. (1988) A two-mirror device for higher harmonic rejection. Nuclear Instruments Methods, 273, 423–428.

Shterenberg, L.E., Aleksandrova, V.A., and Sivtsov, A.V. (1985) Composition, structure and peculiarities in the distribution of Fe, Mn-micronodules in the sediments of the north-eastern Pacific. Litologiya i Poleznye Iskopayemye, 6, 58–70.

Sinha, K.P., and Sinha, A.P.B. (1957) Vacancy distribution and bonding in some oxides of spinel structure. Journal of Physical Chemistry, 61, 758–761.

Stiers, W., and Schwertmann, U. (1985) Evidence for manganese substitution in synthetic goethite. Geochimica et Cosmochimica Acta, 49, 1909–1911.

Strobel, P., Charenton, J.C., and Lenglet, M. (1987) Structural chemistry of phyllomanganates: Experimental evidence and structural models. Revue de Chimie Minérale, 24, 199–220.

Szytula, A., Burewicz, A., Dimitrijevic, Z., Krasnicki, S., Rzany, H., Todorovic, J., Wanic, A., and Wolski, W. (1968) Neutron diffraction studies of α-FeOOH. Physica Status Solidi, 26, 429–434.

Szytula, A., Balanda, M., and Dimitrijevic, A. (1970) Neutron diffraction studies of β-FeOOH. Physica Status Solidi, 3, 1033–1037.

Tamada, O., and Yamamoto, N. (1986) The crystal structure of a new manganese dioxide ($Rb_{0.27}MnO_2$) with a giant tunnel. Mineralogical Journal, 13, 130–140.

Taylor, J.B., and Heiding, R.D. (1958) Arsenates of the transition metals. The arsenates of cobalt and nickel. Canadian Journal of Chemistry, 36, 597–606.

Towe, K.M., and Bradley, W.F. (1967) Mineralogical constitution of colloidal "hydrous ferric oxides." Journal of Colloid and Interface Science, 24, 384–392.

Turner, S., and Buseck, P.R. (1979) Manganese oxide tunnel structures and their intergrowths. Science, 203, 456–458.

Turner, S., and Post, J.E. (1988) Refinement of the substructure and superstructure of romanechite. American Mineralogist, 73, 1155–1161.

Varentsov, I.M., Drits, V.A., Gorhkov, A.I., Sivtsov, A.V., and Sakharov, B.A. (1989) Processes of formation of (Mn,Fe)-crusts in the Atlantic: Mineralogy, geochemistry of basic and trace elements, Krylov Underwater Mountain. In V.N. Kholodov, Ed., Sediment genesis and fundamental problems in lithology, p. 58–78. Nauka, Moscow.

Verwey, E.J.W. (1935) The crystal structure of γ-Fe_2O_3 and γ-Al_2O_3. Zeitschrift für Kristallographie, 91, 65–69.

Vicat, J., Franchon, E., Strobel, P., and Tran Qui, D. (1986) The structure of $K_{1.33}Mn_8O_{16}$ and cation ordering in hollandite-type structures. Acta Crystallographica, B42, 162–167.

Wadsley, A.D. (1952) The structure of lithiophorite, $(Al,Li)MnO_2(OH)_2$. Acta Crystallographica, 5, 676–680.

——— (1953) The crystal structure of psilomelane, $(Ba,H_2O)_2Mn_5O_{10}$. Acta Crystallographica, 6, 433–438.

Waychunas, G.A. (1987) Synchrotron radiation XANES spectroscopy of Ti in minerals: Effects of Ti bonding distances, Ti valence, and site geometry on absorption edge structure. American Mineralogist, 72, 89–101.

Waychunas, G.A., Brown, G.E., Jr., and Apted, M.J. (1983) X-ray K-edge absorption spectra of Fe minerals and model compounds: Near edge structure. Physics and Chemistry of Minerals, 10, 1–9.

Wong, J., Lytle, F.W., Messmer, R.P., and Maylotte, D.H. (1984) K-edge absorption spectra of selected vanadium compounds. Physical Review, B30, 5596–5609.

Manuscript received August 15, 1990
Manuscript accepted July 6, 1992